Fish and Shellfish Immunology 89 (2019) 719–726

Contents lists available at ScienceDirect

Fish and Shellfish Immunology

journal homepage: www.elsevier.com/locate/fsi

Full length article

Spotted knifejaw (*Oplegnathus punctatus*) MyD88: Intracellular localization, signal transduction function and immune responses to bacterial infection

Xiaobing Liu[a], Xuemei Li[a], Xinxin Du[a,c], Minmin Sun[a], Xuangang Wang[a], Wensheng Li[d], Jieming Zhai[d], Jinxiang Liu[a,b], Haiyang Yu[a,b], Quanqi Zhang[a,b,*]

[a] Key Laboratory of Marine Genetics and Breeding, Ministry of Education, College of Marine Life Sciences, Ocean University of China, Qingdao, Shandong, China
[b] Laboratory for Marine Fisheries Science and Food Production Processes, Qingdao National Laboratory for Marine Science and Technology, Qingdao, Shandong, China
[c] Department of Life Science and Engineering, Jining University, Jining, China
[d] LaizhouMingbo Aquatic Co., Ltd., Laizhou, Shandong, China

ARTICLE INFO

Keywords:
MyD88
Immune responses
Signal transduction
Innate immunity
Oplegnathus punctatus

ABSTRACT

Myeloid differentiation factor 88 (MyD88) links members of the toll-like receptor (TLR) and interleukin-1 receptor (IL-1R) superfamily to the downstream activation of NF-κB as a "bridge" molecular in response to exogenous pathogen, but the function in spotted knifejaw (*Oplegnathus. punctatus*), a commercial fish in China, is still unknown. We present a functional analysis of spotted knifejaw MyD88 (OppMyD88) with a typical death domain (DD) at the N-terminus and a conservative Toll/IL-1R (TIR) domain at the C-terminus and suggest that MyD88 is important for the activation of TLR-mediated NF-κB with the synergy between domains. Subcellular localization showed that OppMyD88 was distributed in the cytoplasm in a condensed form. Tissues expression profiling analysis showed that OppMyD88 ubiquitously expressed in all tested tissues with the highest expression in the liver, as determined by real-time PCR. The expression of OppMyD88 significantly upregulated in the liver, spleen, kidney and gills within 120 h post *Vibrio anguillarum* infection. Moreover, we further confirmed that overexpressed OppMyD88 could also induce apoptosis. These results indicate that OppMyD88 might possess important roles in defense against microbial infection and other biological processes in spotted knifejaw similar to those in mammals, which will deepen our understandings in innate immunity of spotted knifejaw.

1. Introduction

Hosts recognition of invading pathogens through gene-encoded pattern recognition receptors (PRRs), the components of innate immune system. PRRs recognize distinct microbial components as pathogen-associated molecular patterns (PAMPs) and activating the immune response. Currently, four different classes of PRR families have been identified in vertebrates. These families include transmembrane proteins such as the Toll-like receptors (TLRs) and C-type lectin receptors (CLRs), as well as cytoplasmic proteins such as the Retinoic acid-inducible gene (RIG)-I-like receptors (RLRs) and NOD-like receptors (NLRs) [1]. The TLR family is one of the best-characterized PRR families which is responsible for sensing invading pathogens outside of the cell and in intracellular endosomes and lysosome [2]. TLRs can induce innate immune responses through association with downstream appropriate adaptor proteins. In mammals, MyD88 is a shared adapter protein of all TLRs, except TLR3, and plays important roles in MyD88-dependent pathways of TLRs signaling transduction [2–6]. Besides the function in innate immunity, MyD88 also mediates TLR2-induced apoptosis via an apoptotic mechanism including Fas-associated death domain protein (FADD) and caspase 8 [7].

MyD88 was originally isolated as one of 12 different mRNA transcripts that were induced in M1 myeloblastic leukemia cells upon activation with lung-conditioned medium or recombinant interleukin (IL)-6 [8]. Latter studies demonstrated that MyD88 plays a vital role in TLR signaling pathway in immune responses. MyD88 contains a death domain in the N-terminus and a TIR domain in the C-terminus, thereby interacting with TLRs. When pathogens bind to TLRs, MyD88 recruits IL-1 receptor-associated kinases (IRAKs) to TLRs through interaction of the death domains of both molecules. IRAKs are activated by phosphorylation and then associate with TRAF6, leading to the activation of the IκB kinase (IKK) complex. The IKK complex induces phosphorylation of IκB, which sequesters the transcription factor NF-κB in the cytoplasm. Degradation of IκB after phosphorylation triggers nuclear translocation of NF-κB to induce expression of inflammatory cytokine genes.

* Corresponding author. No. 5 Yushan Road, Qingdao, Shandong, 266003, China.
E-mail address: qzhang@ouc.edu.cn (Q. Zhang).

https://doi.org/10.1016/j.fsi.2019.04.035
Received 23 January 2019; Received in revised form 2 April 2019; Accepted 11 April 2019
Available online 14 April 2019
1050-4648/

MyD88-deficient mice showed no production of inflammatory cytokines such as TNF-α. IL-6, and IL-12, in response to all TLR ligands [9]. Similarly, research has found that knockout of MyD88 in zebrafish resulted in increased susceptibility to bacteria, and the expression of pro-inflammatory cytokines interleukin (IL)-1β was inhibited [10–12]. Thus, MyD88 is essential for signaling pathways of all TLR family members that lead to the production of inflammatory cytokines. In vitro experiments showed that MyD88 induced the activation of NF-κB and IFN-β, and its function depended on the correct intracellular localization [12–15].

Spotted knifejaw (*O. punctatus*) is an important economic fish species in China and Japan. Good taste, high nutritional value of this fish attract consumers. With the breakthrough of artificial breeding technology, large-scale farming becomes possible. The occurrence of pathogenic diseases has increased greatly as its cultures have expanded. However, knowledge about the immune system of spotted knifejaw is scarce, which hinders the environmentally friendly strategies for disease prevention. Herein, the cDNA sequence of MyD88 of spotted knifejaw was obtained using RT-PCR and RACE-PCR methods and we investigated their expression patterns after *V. anguillarum* challenge. Moreover, the dependence of correct intracellular localization was analyzed. Our results demonstrated the roles of MyD88 in the immune response to bacterial infection in spotted knifejaw and its signal transduction function relies on the correct intracellular localization, which deepens our understanding of the mechanism in innate immune response of spotted knifejaw to bacteria.

2. Materials and methods

2.1. Ethics statement

This study was conducted in accordance with the protocols of the Institutional Animal Care and Use Committee of the Ocean University of China (protocol number 11-06) and the China Government Principles for the Utilization and Care of Vertebrate Animals Used in Testing, Research, and Training (State Science and Technology Commission of the People's Republic of China for No. 2, October 31, 1988. http://www.gov.cn/gongbao/content/2011/content_1860757.htm).

2.2. Fish, V. anguillarum, and cell line

In this study, total 57 healthy six-month old spotted knifejaws (~40 g) were collected from LaiZhou MingBo Aquatic Co., Ltd. (Laizhou, Shandong, China) and cultured for one week in aerated fresh sea water tanks in the experimental station of the Ocean University of China (OUC) before treatment and sampling.

The pathogenic *V. anguillarum* strain LMG 4437(T) was acquired from the Key Laboratory of Microbial Oceanography, OUC. *V. anguillarum* was incubated for 10 h in M2216E medium at 28 °C to reach the mid-logarithmic stage, then used for challenge. Human embryonic kidney cell line (HEK-293T) was cultured in Dulbecco's modified Eagle's medium supplemented with 10% fetal bovine serum and 4 mM L-glutamine at 37 °C in a humidified atmosphere containing 95% air and 5% CO_2.

2.3. In vivo challenge and fish sampling

Before *V. anguillarum* challenge, tissues (liver, spleen, kidney, gill, heat, brain, muscle and intestines) from three healthy individuals were collected for quantitative real-time polymerase chain reaction (qRT-PCR). These samples were used for tissue distribution analysis and as blank control for bacterial challenge. Samples were snap-frozen in liquid nitrogen and stored at −80 °C. Each sample was collected in triplicate.

In the challenge experiment, three healthy individuals above were used as blank controls and the other 54 individuals were equally divided into two groups (named groups A and B). Each group was reared in three independent tanks with volumes of approximately 36 L. The bacteria were suspended in phosphate-buffered saline (PBS, pH = 7.2). Each fish in groups A were intraperitoneally injected with 100 μL of bacterial suspension (5×10^5 colony forming units/mL), while group B were injected with 100 μL of PBS. Three individuals from each group were randomly sampled at 2, 4, 8, 12, 24, 48, 72, 96, and 120 h post injection (hpi). Tissue samples (liver, spleen, kidneys, and gills) were immediately collected, frozen in liquid nitrogen, and then stored at −80 °C until use.

2.4. RNA isolation and cDNA synthesis

Genomic DNA was extracted from dorsal muscles through phenol/chloroform procedure. Total RNA was isolated using Trizol reagent (Invitrogen, USA) according to manufacturer's protocol. Quality and quantity of genomic DNA and total RNA were detected by agarose gel electrophoresis and Nanophotometer Pearl (Implen GmbH, Germany). Then, cDNA was synthesized using a reverse transcriptase M-MLV system (TaKaRa, China).

2.5. Primer design, amplification, and cloning

Partial cDNA sequences of the spotted knifejaw MyD88 gene were obtained using local blast from transcriptome. The 5′ and 3′ end sequences of MyD88 cDNA were amplified using 5′-/3′- full rapid amplification of cDNA ends (RACE) kit (TaKaRa, Dalian, China) following manufacturer's instructions (special amplified primers are shown in

Table 1
Primers used in this study.

Primer name	Primer sequences (5′3′)	Amplification target
MyD88-F	GAGAAAGTAAGAGAGAAAGGCAGC	Amplification of MyD88 partial sequence
MyD88-R	GGCGTCGGAAGGTAAACAG	Amplification of MyD88 partial sequence
MyD88-G-F	GAGAAAGTAAGAGAGAAAGGCAGC	Amplification of MyD88 genome sequence
MyD88-G-R	GGCGTCGGAAGGTAAACAG	Amplification of MyD88 genome sequence
MyD88-5-1	TTCTGAACCCACTTGCCATTTAC	MyD88 5′RACE
MyD88-5-2	GCCTGCCACTACTTTGTATTTATGC	MyD88 5′RACE
MyD88-3-1	TACAGTCCCAACTTCTTCCTCACGC	MyD88 3′RACE
MyD88-3-2	GCTTCAGGCGTCCACAGGTTAC	MyD88 3′ RACE
RACE-UPM	CTAATACGACTCACTATAGGGCAAGCAGTGGTATCAACGCAGAGT	5′ RACE
RACE-NUP	AAGCAGTGGTATCAACGCAGAGT	3′ RACE
MyD88-GFP-F	CCGCTCGAGATGGCGTGTTCCGATCCA	Construction of overexpression vector
MyD88-GFP-R	TCCCCCGCGGCAGTAACTGCCTGGTTGATG	Construction of overexpression vector
MyD88-Q-F	CACGCTTCATAGTTCTGTATCT	Real-time PCR
MyD88-Q-R	GGAAGAAGTTGGGACTGTATC	Real-time PCR
ACTB-Q-F	GGTCTGTGATGCCCTTAGATGTC	Real-time PCR
ACTB-Q-R	AGTGGGGTTCAGCGGGTTAC	Real-time PCR

Table 1). All polymerase chain reaction (PCR) products were ligated into the pMD18-T vector (TaKaRa, Dalian, China) for sequencing. Full-length DNA sequences of MyD88 were assembled by SeqMan software.

2.6. Sequence prediction, alignment, and phylogenetic analysis

Identity analysis of the cDNA sequence with the known sequences published in GenBank was performed using BLASTn (http://blast.ncbi.nlm.nih.gov). DNASTAR multiple program package (DNASTAR Inc., USA) was used to analyze the open reading framework (ORF), putative amino acid sequence, calculated molecular weight, and theoretical isoelectric point. The transmembrane protein was predicted by Tmpred (http://www.ch.embnet.org/software/TMPREDform.html). Protein domains were predicted using the Simple Modular Architecture Research Tool (http://smart.embl-heidelberg.de/). The interaction sites were predicted by NCBI online tool using conserved domains database [16–19]. The three-dimensional (3-D) model of OppMyD88 was deduced with Swiss modeling software provided by the SWISS-MODEL server (https://swissmodel.expasy.org/). The gene structure of MyD88 was predicted by each coding sequence (CDS) and corresponding genomic sequence using the Gene Structure Display Server (http://gsds.cbi.pku.edu.cn/index.php) [20]. MyD88 protein conserved motifs were analyzed by the MEME programs [21]. All the other sequences were downloaded from NCBI websites (species names and accession numbers are available in Table S1).

Alignment of putative amino acid sequences of spotted knifejaw and other known vertebrates was carried out by clustalX2 with the default parameters [22]. Phylogenetic tree was constructed by neighbor-joining method with 1000 bootstrap replicates using MEGA 7.0 [23].

2.7. Quantitative expression analysis of MyD88

MyD88 mRNA expression patterns in different tissues and different time points after *V. anguillarum* challenge were analyzed by qRT-PCR performed with 2 × SYBR Green qPCR Master Mix (Novoprotein, Shanghai, China) using a Roche Light Cycler 480 machine (Roche, Sussex, UK). β-actin was selected as internal control. Relative expression levels of the target gene were expressed as ratios of the target gene copy number to β-actin copy number. Fold changes were expressed as ratios of treated to control groups. qRT-PCR conditions were as follows: pre-denaturation at 95 °C for 30 s, followed by 45 cycles of 95 °C for 15 s, annealing at 60 °C for 45 s. Considering individual genetic variability, samples from three fish were mixed, and each experiment was repeated in triplicate. The relative expressions of MyD88 mRNA were quantified on a relative scale by the $2^{-\Delta\Delta CT}$ method [24].

2.8. Plasmid construction, transfection, and fluorescence microscopy

For overexpression experiments, the complete ORF, Death domain and TIR domain were amplified using specific primer (Table 1) containing the restriction enzyme sites *XhoI* and *SacII*, respectively. The PCR products was inserted into the pEGFP-N1 vector to construct the expression plasmids which were then validated by double enzyme digestion and sequencing.

Before the experiment, a total of 5×10^5 HEK-293T cells were seeded into each wells of 24-well plates and cultured for 24 h. Then, recombined plasmids were transfected into the cells using LipoGene™ 2000 Star Transfection Reagent (US Everbright Inc.) according to the manufacturer's instructions. The control group was transfected with equal amount of pEGFP-N1 vector.

2.9. Dual-luciferase reporter assay

For the dual-luciferase reporter assays, HEK-293T cells were transiently co-transfected with NF-κB reporter vector (100 ng/well), pRL-TK vector (20 ng/well) and targeted recombined vector (500 ng/well). The Renilla luciferase pRL-Tk vector (Promega) was used as an internal control. The cells were lysed at 48 h post-transfection and measured using a luciferase reporter assay system (Promega, USA). Each experiment was repeated six times. To eliminate the influence of the differences in transfection efficiency, the relative luciferase values were calculated by normalized the firefly luciferase activity on basis of activity of the Renilla luciferase activity. The experimental results are expressed as fold stimulation changes relative to the empty vector control.

2.10. Detection of apoptosis

The HEK-293T cells was divided into four groups, which was transfected with OppMyD88-EGFP, OppDeath-EGFP, OppTIR-EGFP and pEGFP-N1 plasmids, respectively. After transfection for 4 h, the cells were cultured in 500 μL DMEM containing 10% FBS at 37 °C with 5% CO_2 for 48 h. Then, the apoptotic cells were detected by a terminal deoxynucleotidyl transferase (TdT)-mediated dUTP nick-end labeling (TUNEL) assay as described previously [25].

2.11. Statistical analysis

The data were statistically analyzed using one-way ANOVA/unpaired Student's t-test by using SPSS 20.0 (IBM, NY, USA). $p < 0.05$ indicated statistical significance between groups. All data were expressed as mean ± standard error of the mean.

3. Results

3.1. Sequence identification and analysis

Full-length MyD88 gene spanned 1728 bp, including a 195 bp 5′ UTR, 888 bp ORF, 645 bp 3′ UTR, and a canonical polyadenylylation signal (^{1678}AATAAA^{1683}) followed by an additional 29 bp by the poly (A) tail (Fig. S1A). The putative protein had a theoretical molecular weight of 33.79 kDa and an isoelectric point of 4.92. Protein domain prediction by Simple Modular Architecture Reach Tool (SMART) revealed that OppMyD88 possesses a death domain at position 12–103 of the amino terminus and a TIR domain at position 152–288 of the carboxyl terminus (Fig. S1B). Further alignments of TIR domain showed that three conserved boxes appeared in all species include fish and tetrapod. Within the death domain, fifteen MyD88-IRAK4 interaction sites were determined by the BLAST program in NCBI (Fig. S1B and C). In TIR domain, three conserved regions known as Box1 (^{153}FDA^{155}), Box2 (^{188}RDVLPG^{193}) and Box3 (^{277}FW^{278}) were observed (Fig. S2A). According to the predicated death and TIR domain of this putative amino acids sequence, OppMyD88 was classified into the MyD88 family.

3.2. Alignment, phylogenetic, and genomic analysis

The deduced amino acid sequence of OppMyD88 was aligned with the known MyD88 from other species by ClustalW, which showed that the OppMyD88 protein shared many protein features with other species (Fig. S2A). The death and TIR domains were the most conserved in the MyD88 protein. Also, the high sequence identity (99.0%–63.1%) of OppMyD88 with other vertebrates suggested that MyD88 is relatively conservative.

SWISS-MODEL workspace was applied to construct the 3-D models. As illustrated in Fig. S2B, the death domain (from 27 aa to 118 aa) and TIR domain (from 169 aa to 303 aa) of OppMyD88 aligned well with all the crystal structures of vertebrate MyD88 death domain and the solution structure of MyD88 TIR, respectively. However, the structure of death domain in invertebrates were changed and helix-1 was lost in *Crassostrea gigas*.

The phylogenetic tree was constructed using MEGA 7.0 based on the

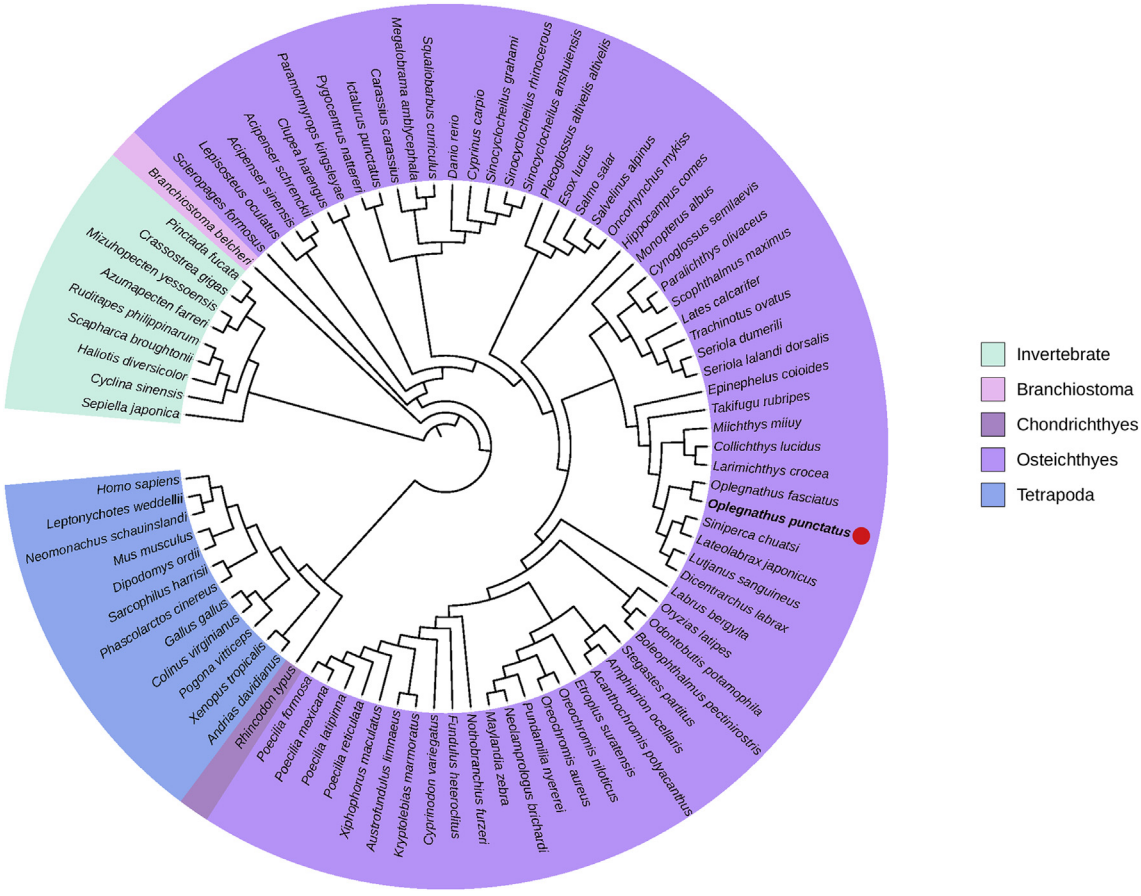

Fig. 1. Phylogenetic relations of OppMyD88 with MyD88 proteins from other species. Phylogenetic tree showing relationships of MyD88 between different species including vertebrate and invertebrate. The phylogenetic tree is constructed by MEGA 7.0 using Neighbor-Joining method with bootstrap value of 1000.

amino acid sequences to study the relationship between OppMyD88 and other species. Phylogenetic analysis demonstrated that the tree was separated into two clusters. The invertebrates was grouped together in the first cluster, and the vertebrates formed the second cluster. OppMyD88 was grouped into the clade of fish MyD88 (Fig. 1). It exhibited the closest relationship to MyD88 from *O. fasciatus*, which belongs to the same genus with *O. punctatus*, followed by other percomorpha fishes.

Comparison of cDNA and DNA sequences was performed to analyze the structure of MyD88 (Fig. S3A). The results revealed that OppMyD88 contained 5 exons and 4 introns. OppMyD88 exhibited the same genomic structure compared with other vertebrates despite the different sequence length. The relative position of exons located in the gene was conserved. Also, conserved motifs of the MyD88 proteins were identified using the MEME program (Fig. S3B). The results showed that 10 conserved putative motifs were identified in most of the vertebrates. The length of the conserved motifs ranged from 4 to 50 amino acids. Furthermore, motif 1, 2, 3, 4, 5 and 7 were conserved in all listed species, which located in the functional domains, Death domain and TIR domain.

3.3. Tissue distribution of OppMyD88 and response to V. anguillarum challenge

According to the relative quantification analysis, OppMyD88 mRNA ubiquitously expressed in the eight tested tissues of spotted knifejaw, but the expression levels differed distinctly among different tissues. The highest level of MyD88 transcript was detected in liver and the lowest in muscle (Fig. 2).

To further learning about the immune functions of OppMyD88, the

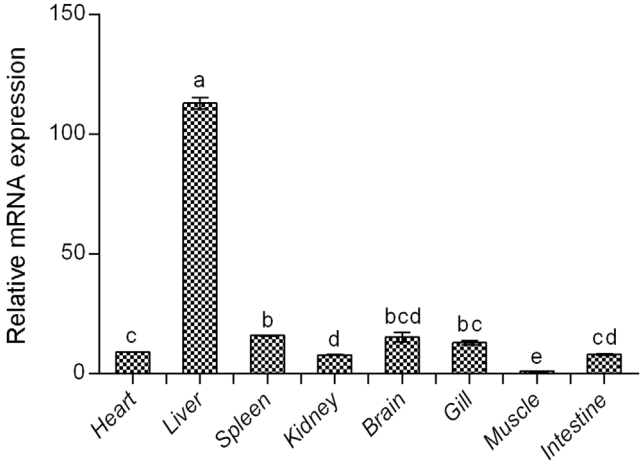

Fig. 2. Distribution of OppMyD88 mRNA in different tissues determined by qRT-PCR. The values are means (± SEM) of three replicates.

expression changes in four classical immune organs, liver, spleen, kidney and gills, were examined after *V, anguillarum* challenge using qRT-PCR. Not surprisingly, the transcripts showed a time dependent expression pattern. In liver, the transcripts was significantly induced to the highest level at 96 hpi with 2.3-fold higher than that of the no-injected group, then decreased to normal level at 120 hpi (Fig. 3A). In spleen, kidney and gills, the highest levels occurred in 12 hpi (~2.6 folds), 8 hpi (~2.1 folds) and 4 hpi (~1.8 folds), respectively (Fig. 3B–D).

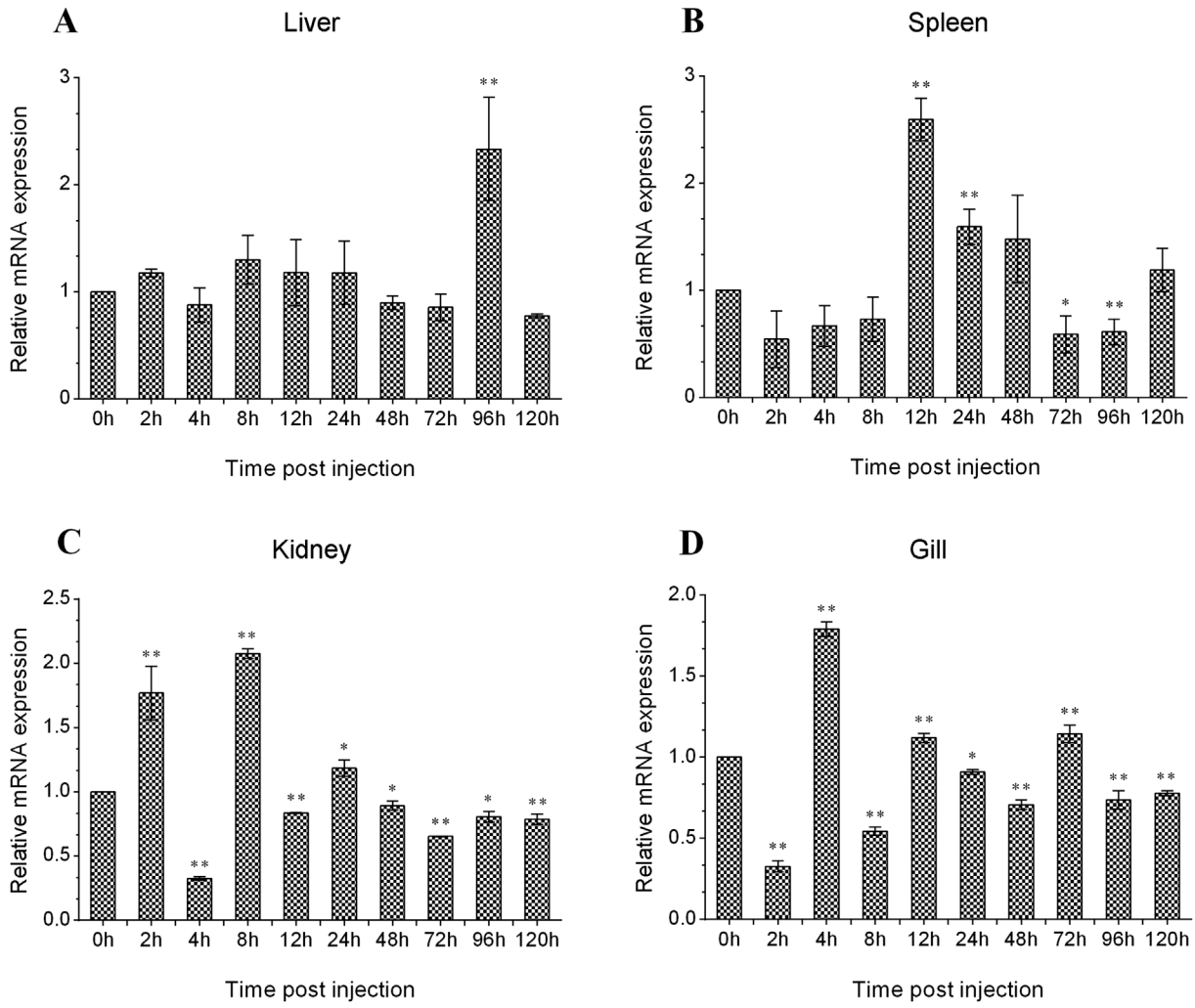

Fig. 3. Immuno responses of OppMyD88 mRNA in liver (A), spleen (B), kidney (C) and gills (D) to *V. anguillarum* challenge at 0, 2, 4, 8, 12, 24, 48, 72, 96 and 120 hpi. Significant differences between the challenged and the control group were indicated with asterisks.

3.4. The localization of OppMyD88 and its effect on activity of NF-κB

The OppMyD88-EGFP plasmids were successfully constructed, verified by sequencing, and transfected to HEK-293T cells. The fusion expression of OppMyD88, enhanced green fluorescent protein (EGFP) tagged at the C-terminal, was detected by fluorescent microscopy. After 24 h, the spotted knifejaw MyD88 was observed distributing in the cytoplasm in a condensed form (Fig. 4). We constructed another two plasmids contained different fluorescences, OppDeath-EGFP and OppTIR-pDsRed which contains the functional domain death domain and TIR domain, respectively. Interestingly, these two fusion proteins were no longer distributed like the OppMyD88-EGFP but distributed all over cytoplasm although some of those fusion proteins still existed in a condensed form (Fig. 5). Moreover, the color of these two fusion proteins were highly overlapped and changed to yellowish green.

To assess the effects of OppMyD88 on NF-κB signaling, the co-

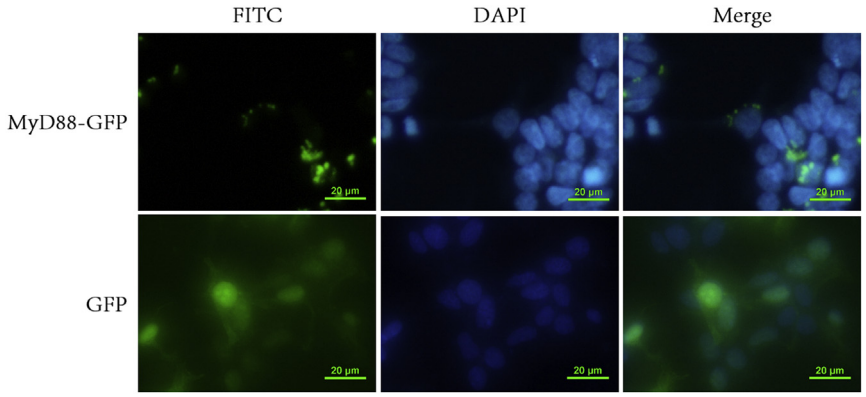

Fig. 4. Subcellular localization of OppMyD88 detected by expressed OppMyD88-EGFP fusion protein in HEK-293T cells using fluorescence microscopy. The distribution of OppMyD88 was observed in cytoplasm of HEK-293T cells.

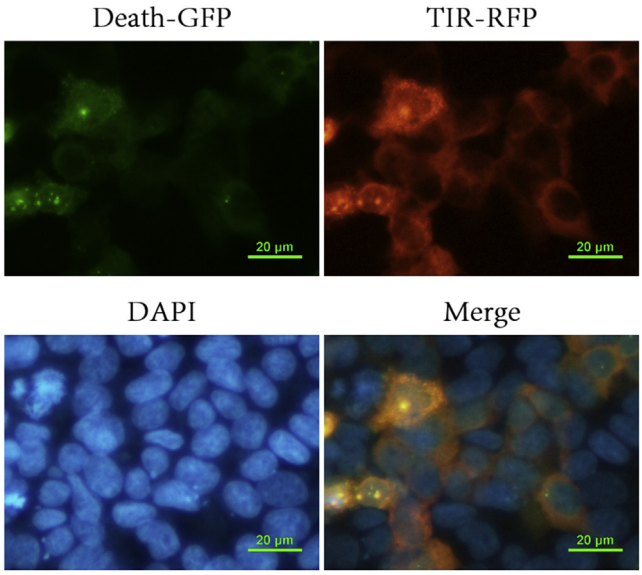

Fig. 5. Subcellular co-localization analysis of OppDeath-EGFP and OppTIR-pDsRed fusion proteins expressed in HEK-293T cells by co-transfection of OppDeath-EGFP and OppTIR-pDsRed plasmids fluorescence microscopy. The co-location were examined using blue and green 40 × lens. (For interpretation of the references to color in this figure legend, the reader is referred to the Web version of this article.)

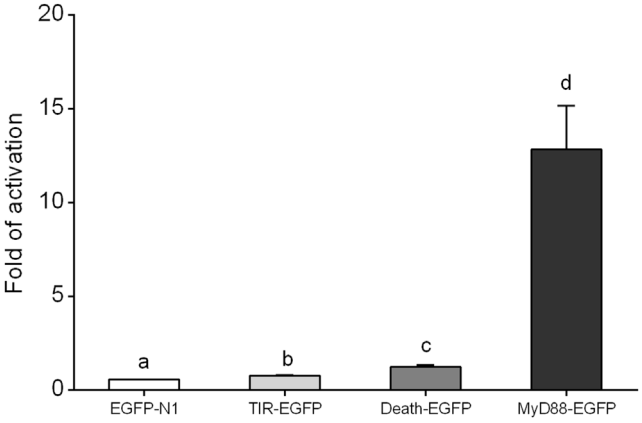

Fig. 6. Effects of OppMyD88, OppDeath and OppTIR on the activity of NF-κB reporter gene. Luciferase activities were tested at 48 h post transfection. Significant differences are indicated by different letters ($p < 0.05$).

transfection assay was performed in the HEK-293T cell line. The results showed that all of the three plasmids could significantly activate the NF-κB compared to the control group. Mentionly, any single domain could not fully activate the NF-κB and only the complete MyD88 protein can activate the NF-κB to a relatively high level (~12.8 folds) (Fig. 6).

3.5. Effects of over-expressed OppMyD88 on apoptosis

In order to investigate the participation of OppMyD88 in the procedures of apoptosis, OppMyD88-EGFP, OppDeath-EGFP and OppTIR-EGFP were transfected into HEK-293T cells, respectively. In the cells untransfected or transfected with control vector (pEGFP-N1) very less apoptosis occurred as revealed by TUNEL assay. In the cells over-expressed OppMyD88, OppDeath and OppTIR significantly increased apoptosis with obviously higher degree of DNA fragmentation were observed (Fig. 7). For details, the numbers of apoptotic cells in OppDeath-EGFP transfection group was similar to the numbers in OppMyD88-EGFP transfection group, while the numbers in OppTIR-EGFP transfection group was markedly less than those two groups above.

4. Discussion

As a kind of crucial adapter protein, MyD88 links members of the toll-like receptor (TLR) and interleukin-1 receptor (IL-1R) superfamily to the downstream activation of nuclear factor-κB and mitogen-activated protein kinases [26]. In the present study, the genome stucture of MyD88 in *O. punctatus* was identified and the 1728 bp full-length cDNA was obtained which contained an ORF of 888 bp encoding a deduced protein of 295 amino acids.

Structural analysis revealed both a conserved death domain homologue at the N-terminal region and a typical TIR domain homologue at the C-terminal region in MyD88, similar with the structure of MyD88 genes from other fish, avian, mammals and invertebrates, suggesting that the function of MyD88 is conservative. In mammals, the TIR domain contains three conserved regions, Box 1, 2 and 3, which play important functions in signal recognition and engaging with downstream elements. It has been proposed that boxes 1 and 2 are involved in the binding of proteins involved in signaling, whereas box 3 is primarily involved in directing localization of receptor, perhaps through interactions with cytoskeletal elements [27]. In our OppMyD88, three conserved functional boxes were also identified in the TIR domain. This result suggested that MyD88 in *O. punctatus* played similar roles as the conserved MyD88 from other species.

The Neighbor-joining tree revealed two major subgroups of MyD88 molecules, one formed by invertebrates, and the other by the branchiostoma, osteichthyes, chondrichthyes and tetrapoda. OppMyD88 clustered with *O. fasciatus* and other teleost species. The result revealed that gene position was generally consistent with the traditional taxonomy for other MyD88 in the different clade. Protein structures determine its functions. Comparative modeling provides a simple method to construct a 3-D structure of the target protein from its amino acids sequence and an experimental 3-D structure of one or more known proteins. Results showed that the 3-D structure of MyD88 death domain and the solution structure of TIR of vertebrates align well with each other, respectively. While the death domain of invertebrate is different from those in vertebrates. Compared to vertebrates, there is a loss of helix-1 in invertebrate, which suggested that in the evolution of invertebrates to vertebrates, structural variation occurred and the structure of MyD88 in different tetrapod animals is relatively conservative.

The expression of MyD88 has been investigated in many species. In mammals, MyD88 expressed in most tissues and organs at different levels [28,29]. In the present study, MyD88 transcript was detected in all tested tissues in spotted knifejaw. The most predominant expression was found in liver and the weakest expression was in muscle. Its expression levels in the gills, spleen and kidney were moderate. MyD88 is a classical molecular participating in the innate immune response. When chanllenged with bacteria or other stimulus such as LPS, PGN, and poly I:C, the expression of MyD88 changed within a few days [30–33]. *V. anguillarum*, a Gram-negative bacterium, is regarded as a cause of serious systemic diseases among cultured spotted knifejaw. In order to explore whether OppMyD88 is involved in antibacterial immunity, fish were infected with *V. anguillarum*. In this study, the variation of MyD88 in spotted knifejaw was detected by qRT-PCR in liver, spleen, kidney and gills after injection. The expression of MyD88 was significantly up-regulated in all the four tissues at different time points compared to control groups, which suggested the important role of MyD88 in response to the *V. anguillarum* infection. After 120 h, the expression levels of MyD88 recovered to normal status in the liver and spleen, suggested steady-state appearance in these tissues. The results in the kidney and gills might mean that pathogen-host interaction was still ongoing and more time needed to remove the pathogenic bacteria in these two tissues. All these results revealed that OppMyD88 is a classical molecule in innate immunity.

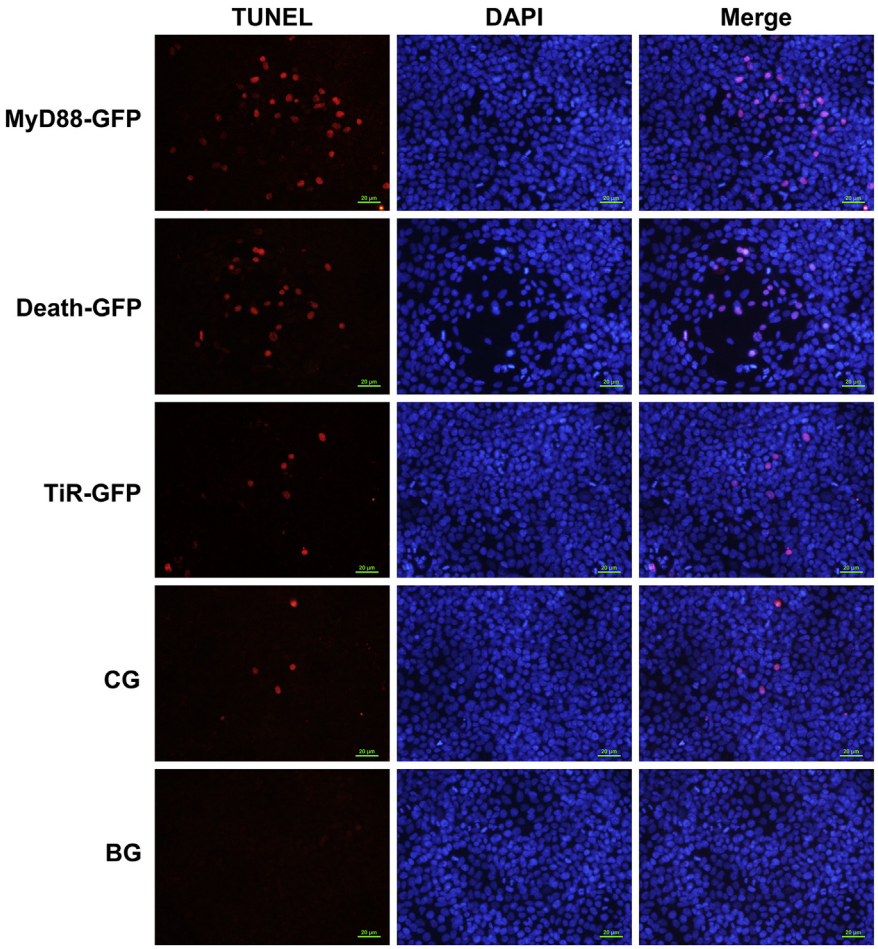

Fig. 7. Effect of OppMyD88 on apoptosis detected by TUNEL assay. The "TUNEL" represents the fractured DNA fragments. The "DAPI" represents the DAPI-stained cell nuclei. The "Merge" represents the combination of cell nuclei and fractured DNA fragments. BG: untransfected blank group; CG: control group transfected with pEGFP-N1. HEK-293T cells transfected with OppMyD88-EGFP, OppDeath-EGFP and OppTIR-EGFP showed higher numbers of fractured DNA fragments.

In all previous studies, MyD88 was identified as a cytoplasmic protein [30,34,35]. Transmembrane analysis showed that OppMyD88 was a non-membrane protein, which correlated with its function as a soluble cytoplasmic molecule. To further assess the functional activity of OppMyD88, the EGFP was tagged at the C-terminal of OppMyD88, which is stably expressed in HEK-293 cells. Significantly increased fluorescence signal was observed in the cytoplasmic region accorded with its role as an adaptor molecule for TLRs. When receiving external stimulation by PAMPs, TLRs molecular conformation changes the interaction through the TIR structure and the cytoplasmic part of the C-end in the TIR domain of MyD88. Upon ligand activation, MyD88 recruits IRAKs and TRAF6. IRAK then becomes phosphorylated and dissociates from MyD88. As a result of this, TRAF6 is activated to trigger downstream cascade reactions resulting in proinflammatory cytokine production [36]. To find out if the localization of OppMyD88 is mediated by a functional domain, the two domains were separated. Interestingly, separated domains of OppMyD88, death domain and TIR domain, mainly distributed in the cytoplasm in a uniform state which is different from the intact protein. These results suggested that the correct subcellular distribution also needs some unknown motifs in the whole amino acid sequence. The overlaped localization of these two domains revealed their functional relevance.

Inflammatory response is the final result of TLR signaling pathway via NF-κB activation [9,37–40]. To date, knowledge about the function of MyD88 on NF-κB activation has been derived from different species, such as *Trionyx sinensis, Crassostrea gigas* and *Larimichthys crocea*, using reporter assays in HEK-293T cells [41–43]. All MyD88s derived from these species above can significantly activate NF-κB. Similar reporter assay was conducted to verify the function of NF-κB activation by MyD88 in *O. punctatus*. As expected, OppMyD88 could significantly activate NF-κB compared to the control group transfected with pEGFP-N1 vector. Moreover, overexpression of Death domain or TIR domain could also activate NF-κB. However, the level of NF-κB activation induced by single functional domain is markedly lower than the intact MyD88 protein. All of the results suggested that single functional domain may undertake partial function of NF-κB activation. In other words, there was no one single domain which undertakes effective function on NF-κB activation. This hypothesis also confirms the subcellular localization results above.

Apart from activating NF-κB, MyD88 could also mediate apoptosis induced by bacterial lipoprotein (BLP)-stimulated TLR2 in human [7]. In TLR2-induced apoptosis, MyD88 binds to Fas-associated death domain protein (FADD) through the interaction of their death domains, and then FADD binds to and activates caspase 8 [7]. Previous studies showed that overexpression of MyD88 was sufficient in inducing apoptosis [7,44]. Our study confirmed that overexpression of OppMyD88 elevated the rate of apoptosis in HEK-293T cells. In the apoptotic process, the death domain in MyD88 is necessary for signal transduction [45]. The over-expression of single death domain of OppMyD88 induced the simlar apoptosis rate in HEK-293T cells as the intact protein, whereas TIR domain induced relatively lower apoptosis rate. These results confirmed the importance of death and TIR domains and indicated that the ability of OppMyD88 in apoptosis relys more on the N-terminal death domain than on TIR domain.

In summary, we identified and characterized the structure, evolutionary status and expression pattern of a MyD88 gene in spotted knifejaw. Immunostimulation experiment revealed that OppMyD88 is a classical molecule participating innate immunity especially in antibacterial immunity. Functional analysis suggested the conserved function between spotted knifejaw and other vertebrates in apoptosis induction and activation of NF-κB. As a cytoplasmic protein, OppMyD88 plays an essential role in innate immunity. These findings may help a further understanding of the functions and evolution of vertebrate MyD88.

Acknowledgements

This work was supported by The Scientific and Technological Innovation Project from Laboratory for Marine Fisheries and Aquaculture, Qingdao National Laboratory for Marine Science and Technology (2015ASKJ02).

Appendix A. Supplementary data

Supplementary data to this article can be found online at https://doi.org/10.1016/j.fsi.2019.04.035.

References

[1] O. Takeuchi, S. Akira, Pattern recognition receptors and inflammation, Cell 140 (6) (2010) 805–820.
[2] S. Akira, S. Uematsu, O. Takeuchi, Pathogen recognition and innate immunity, Cell 124 (4) (2006) 783–801.
[3] P. Bonnert Timothy, E. Garka Kirsten, P. Parnet, G. Sonoda, R. Testa Joseph, E. Sims John, The cloning and characterization of human MyD88: a member of an IL-1 receptor related family 1, FEBS Lett. 402 (1) (1998) 81–84.
[4] E.F. Kenny, L.A.J. O'Neill, Signalling adaptors used by Toll-like receptors: an update, Cytokine 43 (3) (2008) 342–349.
[5] L.A. O'Neill, A.G. Bowie, The family of five: TIR-domain-containing adaptors in Toll-like receptor signalling, Nat. Rev. Immunol. 7 (5) (2007) 353.
[6] A.F. McGettrick, L.A. O'Neill, The expanding family of MyD88-like adaptors in Toll-like receptor signal transduction, Mol. Immunol. 41 (6–7) (2004) 577–582.
[7] A.O. Aliprantis, R.B. Yang, D.S. Weiss, P. Godowski, A.J.T.E.J. Zychlinsky, The apoptotic signaling pathway activated by Toll-like receptor-2, EMBO J 19 (13) (2000) 3325–3336.
[8] K.A. Lord, B. Hoffman-Liebermann, D.A. Liebermann, Complexity of the immediate early response of myeloid cells to terminal differentiation and growth arrest includes ICAM-1, Jun-B and histone variants, Oncogene 5 (3) (1990) 387–396.
[9] S. Akira, K. Takeda, T. Kaisho, Toll-like receptors: critical proteins linking innate and acquired immunity, Nat. Immunol. 2 (2001) 675.
[10] M. van der Vaart, J.J. van Soest, H.P. Spaink, A.H. Meijer, Functional analysis of a zebrafish myd88 mutant identifies key transcriptional components of the innate immune system, Dis. Model. Mech. 6 (3) (2013) 841–854.
[11] A.M. van der Sar, O.W. Stockhammer, C. van der Laan, H.P. Spaink, W. Bitter, A.H. Meijer, MyD88 innate immune function in a zebrafish embryo infection model, Infect. Immun. 74 (4) (2006) 2436–2441.
[12] Y. Liu, M. Li, S. Fan, Y. Lin, B. Lin, F. Luo, C. Zhang, S. Chen, Y. Li, A. Xu, A unique feature of Toll/IL-1 receptor domain-containing adaptor protein is partially responsible for lipopolysaccharide insensitivity in zebrafish with a highly conserved function of MyD88, J. Immunol. 185 (6) (2010) 3391–3400.
[13] S. Yuan, S. Huang, W. Zhang, T. Wu, M. Dong, Y. Yu, T. Liu, K. Wu, H. Liu, M. Yang, An amphioxus TLR with dynamic embryonic expression pattern responses to pathogens and activates NF-κB pathway via MyD88, Mol. Immunol. 46 (11–12) (2009) 2348–2356.
[14] Y. Yan, H. Cui, J. Wei, Y. Huang, X. Huang, Q. Qin, Functional genomic studies on an immune-and antiviral-related gene of MyD88 in orange-spotted grouper, *Epinephelus coioides*, Chin. Sci. Bull. 57 (25) (2012) 3277–3287.
[15] I. Skjæveland, D.B. Iliev, G. Strandskog, J.B. Jørgensen, Identification and characterization of TLR8 and MyD88 homologs in Atlantic salmon (*Salmo salar*), Dev. Comp. Immunol. 33 (9) (2009) 1011–1017.
[16] A. Marchler-Bauer, Y. Bo, L. Han, J. He, C.J. Lanczycki, S. Lu, F. Chitsaz, M.K. Derbyshire, R.C. Geer, N.R. Gonzales, M. Gwadz, D.I. Hurwitz, F. Lu, G.H. Marchler, J.S. Song, N. Thanki, Z. Wang, R.A. Yamashita, D. Zhang, C. Zheng, L.Y. Geer, S.H. Bryant, CDD/SPARCLE: functional classification of proteins via subfamily domain architectures, Nucleic Acids Res. 45 (D1) (2016) D200–D203.
[17] A. Marchler-Bauer, S.H. Bryant, CD-Search: protein domain annotations on the fly, Nucleic Acids Res. 32 (suppl_2) (2004) W327–W331.
[18] A. Marchler-Bauer, M.K. Derbyshire, N.R. Gonzales, S. Lu, F. Chitsaz, L.Y. Geer, R.C. Geer, J. He, M. Gwadz, D.I. Hurwitz, C.J. Lanczycki, F. Lu, G.H. Marchler, J.S. Song, N. Thanki, Z. Wang, R.A. Yamashita, D. Zhang, C. Zheng, S.H. Bryant, CDD: NCBI's conserved domain database, Nucleic Acids Res. 43 (D1) (2014) D222–D226.
[19] A. Marchler-Bauer, S. Lu, J.B. Anderson, F. Chitsaz, M.K. Derbyshire, C. DeWeese-Scott, J.H. Fong, L.Y. Geer, R.C. Geer, N.R. Gonzales, M. Gwadz, D.I. Hurwitz, J.D. Jackson, Z. Ke, C.J. Lanczycki, F. Lu, G.H. Marchler, M. Mullokandov, M.V. Omelchenko, C.L. Robertson, J.S. Song, N. Thanki, R.A. Yamashita, D. Zhang, N. Zhang, C. Zheng, S.H. Bryant, CDD: a Conserved Domain Database for the functional annotation of proteins, Nucleic Acids Res. 39 (suppl_1) (2010) D225–D229.
[20] B. Hu, J. Jin, A.-Y. Guo, H. Zhang, J. Luo, G. Gao, GSDS 2.0: an upgraded gene feature visualization server, Bioinformatics 31 (8) (2015) 1296–1297.
[21] T.L. Bailey, N. Williams, C. Misleh, W.W. Li, MEME: discovering and analyzing DNA and protein sequence motifs, Nucleic Acids Res. 34 (2006) W369–W373 (Web Server issue).
[22] R. Chenna, H. Sugawara, T. Koike, R. Lopez, T.J. Gibson, D.G. Higgins, J.D. Thompson, Multiple sequence alignment with the Clustal series of programs, Nucleic Acids Res. 31 (13) (2003) 3497–3500.
[23] G. Stecher, S. Kumar, K. Tamura, MEGA7: molecular evolutionary genetics analysis version 7.0 for bigger datasets, Mol. Biol. Evol. 33 (7) (2016) 1870–1874.
[24] K.J. Livak, T.D.J.m. Schmittgen, Analysis of relative gene expression data using real-time quantitative PCR and the $2-\Delta\Delta CT$ method, Methods 25 (4) (2001) 402–408.
[25] C. Ren, T. Chen, H. Sun, X. Jiang, C. Hu, J. Qian, Y. Wang, The first echinoderm poly-U-binding factor 60 kDa (PUF60) from sea cucumber (*Stichopus monotuberculatus*): molecular characterization, inducible expression and involvement of apoptosis, Fish Shellfish Immunol 47 (1) (2015) 196–204.
[26] S. Janssens, R. Beyaert, A universal role for MyD88 in TLR/IL-1R-mediated signaling, Trends Biochem. Sci. 27 (9) (2002) 474–482.
[27] J.L. Slack, K. Schooley, T.P. Bonnert, J.L. Mitcham, E.E. Qwarnstrom, J.E. Sims, S.K. Dower, Identification of two major sites in the type I interleukin-1 receptor cytoplasmic region responsible for coupling to pro-inflammatory signaling pathways, J. Biol. Chem. 275 (7) (2000) 4670–4678.
[28] K. Burns, F. Martinon, C. Esslinger, H. Pahl, P. Schneider, J.L. Bodmer, F. Di Marco, L. French, J. Tschopp, MyD88, an adapter protein involved in interleukin-1 signaling, J. Biol. Chem. 273 (20) (1998) 12203–12209.
[29] S. Janssens, K. Burns, J. Tschopp, R.J.C.B. Beyaert, Regulation of interleukin-1-and lipopolysaccharide-induced NF-κB activation by alternative splicing of MyD88, Curr. Biol. 12 (6) (2002) 467–471.
[30] W.S. Huang, Z.X. Wang, Y. Liang, P. Nie, B. Huang, Characterization of MyD88 in Japanese eel, *Anguilla japonica*, Fish Shellfish Immunol. 81 (2018) 374–382.
[31] L. Huo, M. Bao, Z. Lv, C. Chi, T. Wang, H. Liu, Identification, functional characterization and expression pattern of myeloid differentiation factor 88 (MyD88) in *Sepiella japonica*, Fish Shellfish Immunol. 79 (2018) 112–119.
[32] B. Guo, S. Liu, J. Li, Z. Liao, H. Liu, H. Xia, P. Qi, Identification and functional characterization of three myeloid differentiation factor 88 (MyD88) isoforms from thick shell mussel *Mytilus coruscus*, Fish Shellfish Immunol. 83 (2018) 123–133.
[33] L. Qiu, L. Song, Y. Yu, W. Xu, D. Ni, Q. Zhang, Identification and characterization of a myeloid differentiation factor 88 (MyD88) cDNA from Zhikong scallop *Chlamys farreri*, Fish Shellfish Immunol. 23 (3) (2007) 614–623.
[34] L. Huo, M. Bao, Z. Lv, C. Chi, T. Wang, H. Liu, Identification, functional characterization and expression pattern of myeloid differentiation factor 88 (MyD88) in *Sepiella japonica*, Fish Shellfish Immunol. 79 (2018) 112–119.
[35] Y.-W. Li, Z. Wang, Z.-Q. Mo, X. Li, X.-C. Luo, X.-M. Dan, A.-X. Li, Grouper (*Epinephelus coioides*) MyD88 and Tollip: intracellular localization and signal transduction function, Fish Shellfish Immunol. 42 (1) (2015) 153–158.
[36] T. Kawai, S. Akira, TLR signaling, Cell Death Differ 13 (5) (2006) 816.
[37] C.E. Bryant, M. Symmons, N.J. Gay, Toll-like receptor signalling through macromolecular protein complexes, Mol. Immunol. 63 (2) (2015) 162–165.
[38] A. Goto, J.-L. Imler, Toll signaling in flies and mammals: two sorts of MyD88, Immunity 36 (4) (2012) 555–557.
[39] J. Krishnan, K. Selvarajoo, M. Tsuchiya, G. Lee, S. Choi, Toll-like receptor signal transduction, Exp. Mol. Med. 39 (2007) 421.
[40] M. Schnare, G.M. Barton, A.C. Holt, K. Takeda, S. Akira, R. Medzhitov, Toll-like receptors control activation of adaptive immune responses, Nat. Immunol. 2 (2001) 947.
[41] X. Li, B. Zhu, N. Chen, H. Hu, J. Chen, X. Zhang, J. Li, W. Fang, Molecular characterization and functional analysis of MyD88 in Chinese soft-shelled turtle *Trionyx sinensis*, Fish Shellfish Immunol. 30 (1) (2011) 33–38.
[42] I. Skjæveland, D.B. Iliev, G. Strandskog, J.B. Jørgensen, Identification and characterization of TLR8 and MyD88 homologs in Atlantic salmon (*Salmo salar*), Dev. Comp. Immunol 33 (9) (2009) 1011–1017.
[43] X. Tang, B. Huang, L. Zhang, L. Li, G. Zhang, Molecular characterization of Pacific oyster (*Crassostrea gigas*) IRAK4 gene and its role in MyD88-dependent pathway, Dev. Comp. Immunol. 72 (2017) 21–29.
[44] F. Jaunin, K. Burns, J. Tschopp, T.E. Martin, S. Fakan, Ultrastructural distribution of the death-domain-containing MyD88 protein in HeLa cells, Exp. Cell. Res. 243 (1) (1998) 67–75.
[45] N. Itoh, S. Nagata, A novel protein domain required for apoptosis. Mutational analysis of human Fas antigen, J. Biol. Chem. 268 (15) (1993) 10932–10937.